

University of Groningen

## Carbon dioxide characteristics of water masses in the northern North Atlantic Ocean

Stoll, M.H.C.; Aken, H.M. van; Baar, H.J.W. de; Kraak, M.

*Published in:*  
Marine Chemistry

*DOI:*  
[10.1016/S0304-4203\(96\)00058-8](https://doi.org/10.1016/S0304-4203(96)00058-8)

**IMPORTANT NOTE:** You are advised to consult the publisher's version (publisher's PDF) if you wish to cite from it. Please check the document version below.

*Document Version*  
Publisher's PDF, also known as Version of record

*Publication date:*  
1996

[Link to publication in University of Groningen/UMCG research database](#)

*Citation for published version (APA):*

Stoll, M. H. C., Aken, H. M. V., Baar, H. J. W. D., & Kraak, M. (1996). Carbon dioxide characteristics of water masses in the northern North Atlantic Ocean. *Marine Chemistry*, 55(3), 217-232.  
[https://doi.org/10.1016/S0304-4203\(96\)00058-8](https://doi.org/10.1016/S0304-4203(96)00058-8)

**Copyright**

Other than for strictly personal use, it is not permitted to download or to forward/distribute the text or part of it without the consent of the author(s) and/or copyright holder(s), unless the work is under an open content license (like Creative Commons).

The publication may also be distributed here under the terms of Article 25fa of the Dutch Copyright Act, indicated by the "Taverne" license. More information can be found on the University of Groningen website: <https://www.rug.nl/library/open-access/self-archiving-pure/taverne-amendment>.

**Take-down policy**

If you believe that this document breaches copyright please contact us providing details, and we will remove access to the work immediately and investigate your claim.

*Downloaded from the University of Groningen/UMCG research database (Pure): <http://www.rug.nl/research/portal>. For technical reasons the number of authors shown on this cover page is limited to 10 maximum.*

# Carbon dioxide characteristics of water masses in the northern North Atlantic Ocean

M.H.C. Stoll, H.M. van Aken, H.J.W. de Baar, M. Kraak

*Netherlands Institute for Sea Research, P.O. Box 59, NL-1790 AB Den Burg (Texel), The Netherlands*

Received 20 March 1995; accepted 28 March 1996

---

## Abstract

Accurate measurements of total dissolved carbon dioxide ( $\text{TCO}_2$ ) together with other tracers ( $\theta$ ,  $S$ ,  $\text{O}_2$ , and nutrients) have been carried out during a hydrographic survey of a zonal section between Ireland and Greenland and a number of sections in the Iceland Basin. The resulting data, with  $> 1300$   $\text{TCO}_2$  data points, have allowed the determination of the  $\text{TCO}_2$  signature of the water masses in the northern North Atlantic Ocean in terms of seven water types. The structure of  $\text{TCO}_2$  and dissolved phosphate and nitrate appears to be well correlated with the apparent oxygen utilization. This indicates that ageing of the water types, by mineralization of organic matter, is more important for the observed  $\text{TCO}_2$  structure than differences in the preformed  $\text{TCO}_2$  when the water types were formed. The overturning of water in the “oceanic conveyor belt” will support meridional  $\text{TCO}_2$  transport. This transport was estimated at  $0.16 \cdot 10^6 \text{ mol s}^{-1}$  ( $-0.06 \text{ Gt a}^{-1} \text{ C}$ ) from the differences of  $\text{TCO}_2$  content between the northward flowing Surface and Sub-Polar Mode water and the southward flowing deep Iceland–Scotland and Denmark Strait Overflow Waters.

**Keywords:** hydrography;  $\text{TCO}_2$ ; North Atlantic

---

## 1. Introduction

The northern North Atlantic Ocean exerts considerable influence on the global climate system. The net loss of heat to the atmosphere affects air temperature at higher latitudes, but also drives the formation of cold, deep-water types. The southward thermohaline transport of the North Atlantic Deep-Water Complex is compensated by a net northward transport of warmer surface waters in the wind-driven sub-Arctic cyclonic gyre. If the spatially variable distribution of total dissolved carbon dioxide ( $\text{TCO}_2$ ) correlates with the thermohaline and wind-driven current field, the ocean circulation in this area may support a meridional transport of  $\text{TCO}_2$  via the

so-called “oceanic conveyor belt” (Broecker and Peng, 1982). For example, Brewer et al. (1989) estimated the meridional northward ( $63.9 \cdot 10^6 \text{ mol s}^{-1}$ ) and southward ( $-64.6 \cdot 10^6 \text{ mol s}^{-1}$ ) fluxes of  $\text{TCO}_2$  across the  $25^\circ\text{N}$  latitude in the Atlantic Ocean and arrived at a net southward transport (pre-industrial + anthropogenic) of  $-0.7 \cdot 10^6 \text{ mol s}^{-1}$  (or  $-0.26 \pm 0.03 \text{ Gt a}^{-1} \text{ C}$ ). Martel and Wunsch (1993) suggest that this transport estimate does not differ statistically significant from zero because of a too large uncertainty of the  $\text{TCO}_2$  concentration as a function of position and an additional uncertainty in the circulation. Tans et al. (1990) reckoned the North Atlantic Ocean (sub-tropical gyre between  $15^\circ\text{N}$  and  $50^\circ\text{N}$  and the North Atlantic Ocean and Arctic and

Polar seas north of 50°N) to take up atmospheric CO<sub>2</sub> at a rate of 0.53 Gt a<sup>-1</sup> C, of which an unknown part is the pre-industrial (steady state) uptake. Broecker and Peng (1992) assess the pre-industrial net southward cross-equatorial transport to be  $-1.4 \cdot 10^{-6}$  mol s<sup>-1</sup> ( $-0.6$  Gt a<sup>-1</sup> C) which on its own is already larger than the (pre-industrial + anthropogenic) estimate of Tans et al. (1990).

Obviously an accurate understanding of the TCO<sub>2</sub> content, and its spatial distribution in relation to the distribution, of the various North Atlantic water types is a prerequisite for the assessment of the oceanic CO<sub>2</sub> budgets, and of the role of the different water types for the meridional carbon transport. Here we present for the first time an accurate characterization of the hydrographic structure of TCO<sub>2</sub> in the water masses in the northern North Atlantic Ocean, relying on an accurate and extensive data set of TCO<sub>2</sub> (> 1300 samples) and other hydrographic tracers as determined during the DUTCH-WARP programme in 1991 on board RV "Tyro". A zonal section from the Irish continental shelf towards Greenland (WOCE Hydrographic Programme repeat section AR7E, nominal station distance 30 nautical miles) was combined with several high-resolution sections (nominal station distance 15 nautical miles) south of Iceland (Fig. 1). On the AR7E section water samples from

all 24 Niskin bottles were used for the determination of TCO<sub>2</sub>. The resulting vertical resolution varied from  $\leq 200$  m at the mid-levels of the water column to 50 m in the near-surface and near-bottom layers. On the high-resolution sections in the Iceland Basin only 12 TCO<sub>2</sub> samples per cast were drawn. All TCO<sub>2</sub> data were obtained by coulometry with a precision of  $\pm 1.3$   $\mu$ mol kg<sup>-1</sup> and an accuracy of  $\sim \pm 2$   $\mu$ mol kg<sup>-1</sup>. There exists a smaller data set (TTO-NAS from 1981) for a zonal section between Ireland and Greenland, based on acid titration TCO<sub>2</sub> determinations with inherently lower precision ( $\sim 7$ – $9$   $\mu$ mol kg<sup>-1</sup>; Brewer et al., 1989; Stoll et al., 1993). The earlier GEOSECS data set does not contain CO<sub>2</sub> results for its stations 1 to 23 in the Iceland region. Brewer et al. (1989) reckon the TTO-NAS data set to suffer from systematic offsets due to interfering organic matter. However, from comparing > 400 duplicates sampled during JGOFS cruises in 1989 and 1990, analysed by both coulometry and acid titration Stoll et al. (1993) find good agreement between both methods. The TTO data set being accepted, its inherent precision ( $\pm 7$ – $9$   $\mu$ mol kg<sup>-1</sup> by acid titration) is less though than for the current study ( $\pm 1$ – $2$   $\mu$ mol kg<sup>-1</sup> by coulometry). The flux estimates, mentioned above are partly (Brewer et al., 1989) or largely (Broecker and Peng, 1992) based on

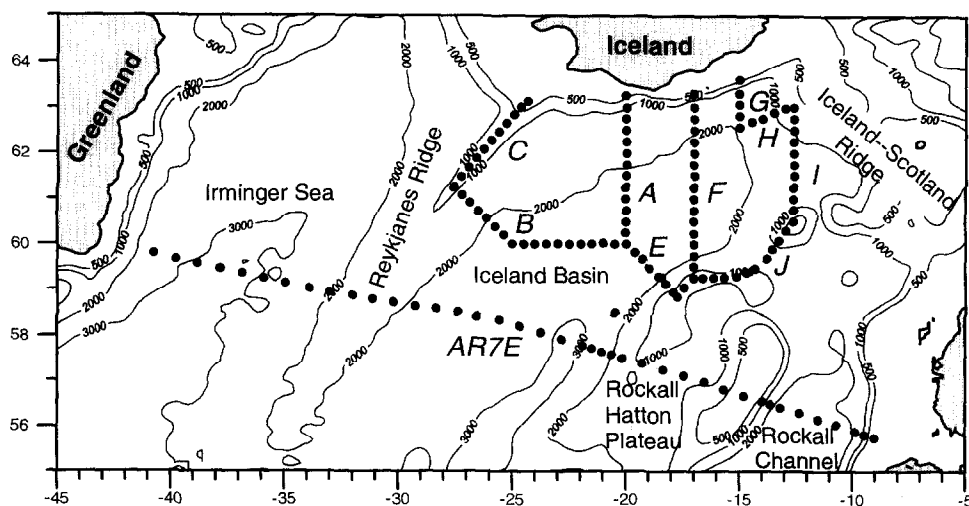


Fig. 1. Position of the hydrographic stations and sections occupied during the DUTCH-WARP cruise of RV "Tyro" in April/May 1991. The depth of the isobaths is indicated in meters.

data sets with the less precise acid titration values, as the more precise coulometry only recently has become available.

The wind-driven circulation brings warm and saline Atlantic Surface Water and Sub-Polar Mode Water from the North Atlantic Current into the Iceland Basin and further northwards to the regions of actual deep-water formation. The resulting density difference between the Arctic seas and the North Atlantic Ocean drives a deep return flow across the sills between these ocean areas. Iceland–Scotland Overflow Water flows through the Faroe Bank Channel and across the Iceland–Faroe Ridge into the Iceland Basin, while Denmark Strait Overflow Water flows through Denmark Strait into the Irminger Sea. This cold overflow water in the Atlantic Ocean is topographically guided by the Icelandic slope, the Reykjanes Ridge and the Greenland slope, and affected by entrainment of recirculating deep-water types in both the Iceland Basin and in the Irminger Basin (Dickson et al., 1990; Dickson and Brown, 1994; Van Aken and De Boer, 1995). The use of salinity, potential temperature and nutrients is essential to describe the flow patterns and to understand and quantify the mixing of these interacting water types (Van Aken and De Boer, 1995). The accurate coulometric  $\text{TCO}_2$  results enable us for the first time to assess the hydrographic structure of the  $\text{TCO}_2$  distribution and its importance for the meridional advective flux of dissolved inorganic carbon.

## 2. Methods

Seawater samples were collected in Niskin bottles at the stations occupied during the DUTCH-WARP cruise of RV “Tyro” along 10 sections in April/May 1991 (Fig. 1). Concurring parameters derived from the CTD sensors were temperature, potential temperature ( $\theta$ ) and salinity ( $S$ ) and pressure ( $P$ ) following data processing and calibrations as described by Van Aken (1992). From the Niskin bottles samples were drawn for the analysis of dissolved oxygen ( $\text{O}_2$ ), total carbon dioxide ( $\text{TCO}_2$ ), and the dissolved nutrients silica ( $\text{Si}$ ), nitrate ( $\text{NO}_3$ ), and phosphate ( $\text{PO}_4$ ).

The  $\text{O}_2$  concentrations were measured with a high-precision automated photometric Winkler titra-

tion and their precision is estimated to be better than  $\pm 0.5 \mu\text{mol kg}^{-1}$ , the accuracy is  $\pm 0.5 \mu\text{mol kg}^{-1}$ . The nutrients were analysed with a TRAACS auto-analyzer and their precision is  $\pm 0.08 \mu\text{mol kg}^{-1}$  for  $\text{Si}$ ,  $\pm 0.11 \mu\text{mol kg}^{-1}$  for  $\text{NO}_3$  and  $\pm 0.07 \mu\text{mol kg}^{-1}$  for  $\text{PO}_4$ . Their accuracy is  $\pm 0.11$ ,  $\pm 0.14$  and  $\pm 0.09 \mu\text{mol kg}^{-1}$ , respectively, as determined from laboratory prepared standards. The  $\text{TCO}_2$  values were determined by coulometry with an automated extraction line (Johnson et al., 1987; Robinson and Williams, 1991; Stoll, 1994) with a precision of  $\pm 1.3 \mu\text{mol kg}^{-1}$  and an accuracy of  $\sim \pm 2 \mu\text{mol kg}^{-1}$ . The accuracy was assessed by means of  $\text{Na}_2\text{CO}_3$  standards.

Obvious outliers from our  $\text{TCO}_2$  data were inspected and almost always found to be low values in  $\text{TCO}_2$  in surface waters correlating with low values in nutrients, especially of  $\text{Si}$ , and high values in  $\text{O}_2$ , indicative of the relative importance of primary production in early spring blooms of diatoms. Only three outlier values remained unaccounted for and were removed from the  $\text{TCO}_2$  data set which now consists of 1375 values. The absolute  $\text{TCO}_2$  values of this study are in fair agreement with the TTO data from the Iceland Basin, and with (mostly preliminary) data from colleagues taken at stations in the Iceland Basin (1989 US JGOFS at  $\sim 60^\circ\text{N}$ ,  $20^\circ\text{W}$ ; 1989–1991 UK-BOFS at  $\sim 60^\circ\text{N}$ ,  $20^\circ\text{W}$ ; NL-JGOFS at  $\sim 60^\circ\text{N}$ ,  $20^\circ\text{W}$ ; Gislefoss, unpublished results, 1992; Schneider, unpublished results, 1992). Earlier work of Chen et al. (1990) north of Iceland was reported as excess  $\text{TCO}_2$  hence not directly comparable, although the given values appear similar.

## 3. Water types and their characteristics

The hydrographic structure of the water masses in the northern North Atlantic has been described extensively by Van Aken and De Boer (1995). Here we will summarize and extend their results and discuss the hydrographic structure with the help of plots (Figs. 2 and 3) of properties vs. the potential temperature ( $\theta$ ), as well as with sections of property distributions along section AR7E (Fig. 4) at a nominal latitude of  $58^\circ\text{N}$  and along section F (Fig. 5) at a longitude of  $17^\circ\text{W}$ . In the  $\theta$ -property plots the approximate positions of the water types are indi-

cated with a number. The acronyms for the water types, as used in this paper and the characteristic observed hydrographic properties of these water types are summarized in Table 1.

### 3.1. The surface layer

The properties of the surface water (SW, 1) are generally determined by atmospheric forcing, and by biological processes in the photic zone (algal

blooms). Section AR7E was surveyed in early spring from 12 to 22 April, when hardly any seasonal stratification was observed. Along this section the sea surface temperature varied from well over 9.5°C in the Rockall Channel to slightly over 3.5°C in the centre of the Irminger Sea (Fig. 4a), well correlated with the sea surface salinity (Fig. 4b). The highest sea surface temperatures and salinities, indicative for the core of water from the North Atlantic Current were found in the Rockall Channel (Fig. 4a and b)

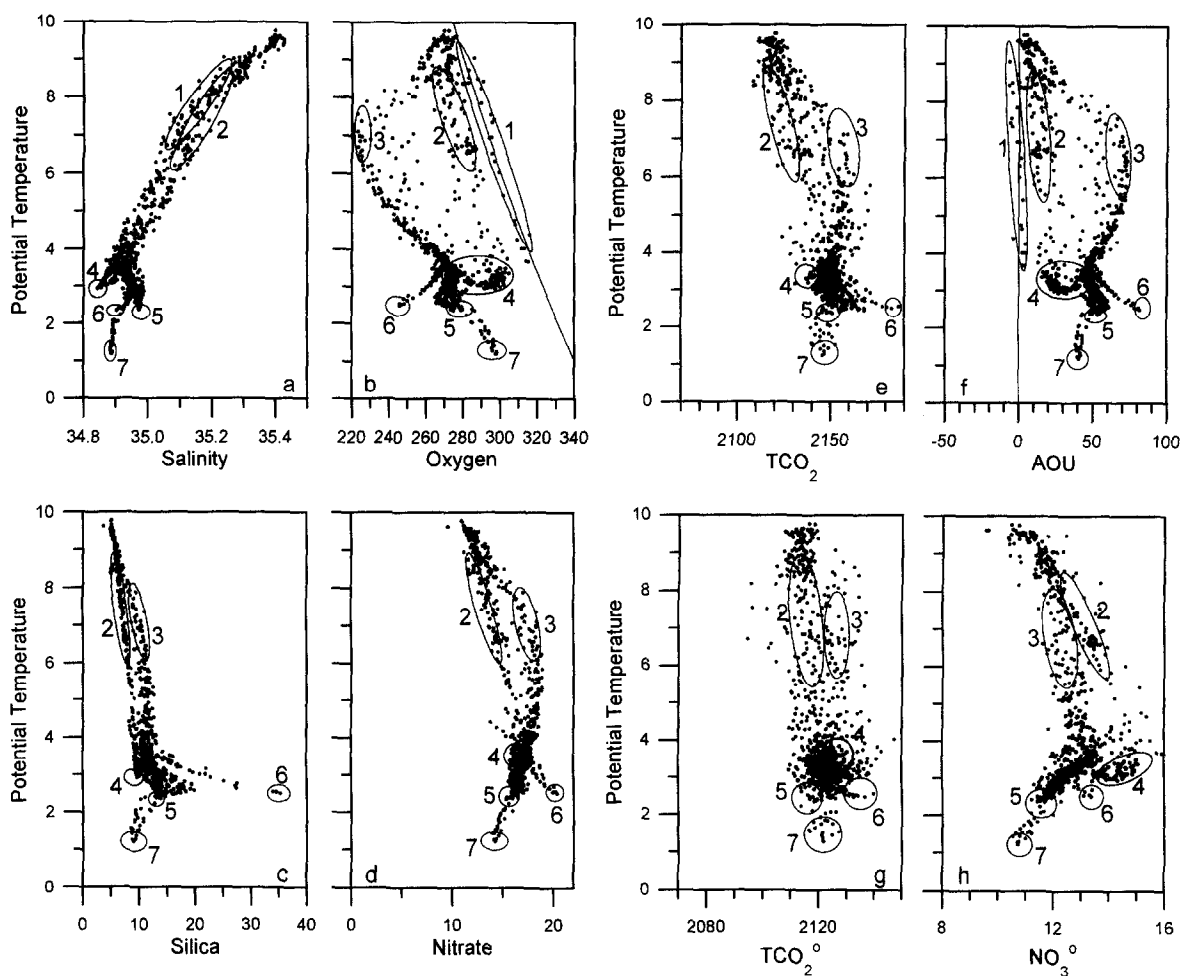


Fig. 2.  $\theta$ -property plots of all samples on section AR7E between Ireland and Greenland: (a)  $\theta$ -S plot; (b)  $\theta$ -O<sub>2</sub> plot; (c)  $\theta$ -Si plot; (d)  $\theta$ -NO<sub>3</sub> plot; (e)  $\theta$ -TCO<sub>2</sub> plot; (f)  $\theta$ -AOU plot; (g)  $\theta$ -TCO<sub>2</sub><sup>0</sup> plot; and (h)  $\theta$ -NO<sub>3</sub><sup>0</sup> plot.  $\theta$  is given in (°C), while the biogeochemical parameters are given in  $\mu\text{mol kg}^{-1}$ . The approximate positions of the water types is indicated with ellipses which are identified with a number according to Table 1. 1 = Surface Water; 2 = Sub-Polar Mode Water; 3 = Intermediate Water; 4 = Labrador Sea Water; 5 = Iceland-Scotland Overflow Water; 6 = Lower Deep Water; and 7 = Denmark Strait Overflow Water.

Table 1  
Hydrographic characteristics of water types in the northern North Atlantic Ocean, as observed in April/May 1991

No.	Water type	$\theta$ (°C)	S	O <sub>2</sub> ( $\mu\text{mol kg}^{-1}$ )	Si ( $\mu\text{mol kg}^{-1}$ )	NO <sub>3</sub> ( $\mu\text{mol kg}^{-1}$ )	TCO <sub>2</sub> ( $\mu\text{mol kg}^{-1}$ )	AOU ( $\mu\text{mol kg}^{-1}$ )	TCO <sub>2</sub> <sup>0</sup> ( $\mu\text{mol kg}^{-1}$ )	NO <sub>3</sub> <sup>0</sup> ( $\mu\text{mol kg}^{-1}$ )
1	Surface Water (SW)	3.5–9.5	34.9–35.4	270–315	5.0–9.5	11.0–16.0	2110–2140	–6 to 6	2110–2145	10.5–15.5
2	Sub-Polar Mode Water (SPMW)	3.5–9.0	34.90–35.35	260–305	5.0–10.0	11.5–16.0	2120–2150	5 to 20	2110–2140	11.5–14.5
3	Intermediate Water (IW)	6.5	35.1	220	10.0	18.5	2170	70	2128	12.5
4	Labrador Sea Water (LSW)									
	Irminger Sea	2.9	34.84	297	9.7	16.7	2143	25	2128	14.6
	Iceland Basin	3.4	34.89	280	10.5	16.7	2141	41	2116	13.1
	Rockall Channel	3.5	34.92	272	12.3	17.2	2146	47	2118	13.1
5	Iceland–Scotland Overflow Water (ISOW)	2.0	35.00	286	9.3	14.8	2142	46	2114	10.9
6	Lower Deep Water (LDW)	2.5	34.94	246	35.3	20.4	2183	82	2134	13.4
7	Denmark Strait Overflow Water (DSOW)	1.2	34.89	298	9.0	14.2	2145	40	2121	10.8

For the determination of SW properties the stations clearly showing effects of a spring bloom have been excluded.

and on the northern side of the Rockall Hatton Plateau (Fig. 5a and b). The sections in the Iceland Basin were surveyed in the last week of April and the first two weeks of May, during the onset of the seasonal stratification. The mean sea surface  $O_2$  concentration along AR7E was only slightly under-saturated with an apparent oxygen utilization (AOU, defined in the following section) of  $1.1 \mu\text{mol kg}^{-1}$ ; standard deviation  $3.8 \mu\text{mol kg}^{-1}$  (Fig. 2b and f) while it was on average well over-saturated during the survey of the Iceland Basin; mean  $AOU = -9.4 \mu\text{mol kg}^{-1}$ , standard deviation  $\pm 11.9 \mu\text{mol kg}^{-1}$  (Figs. 3b, f and 5e). The high  $O_2$  values in the SW

concurred with low nutrient values (Fig. 3c and d), especially Si, indicative for the onset of the spring diatom bloom in the end of April.

The sub-surface water in the upper layers of the northern North Atlantic is designated Sub-Polar Mode Water (SPMW, 2) following McCartney and Talley (1982). In winter this water type reaches to the sea surface and is in direct contact with the atmosphere, due to deep convective mixing driven by surface cooling, which causes relatively weak vertical gradients in  $\Theta$  and  $S$ . The depth of the SPMW layer reaches from  $\sim 200$  m along the edges of the Irminger Sea (Fig. 4a and b) to 800 m in the Rockall

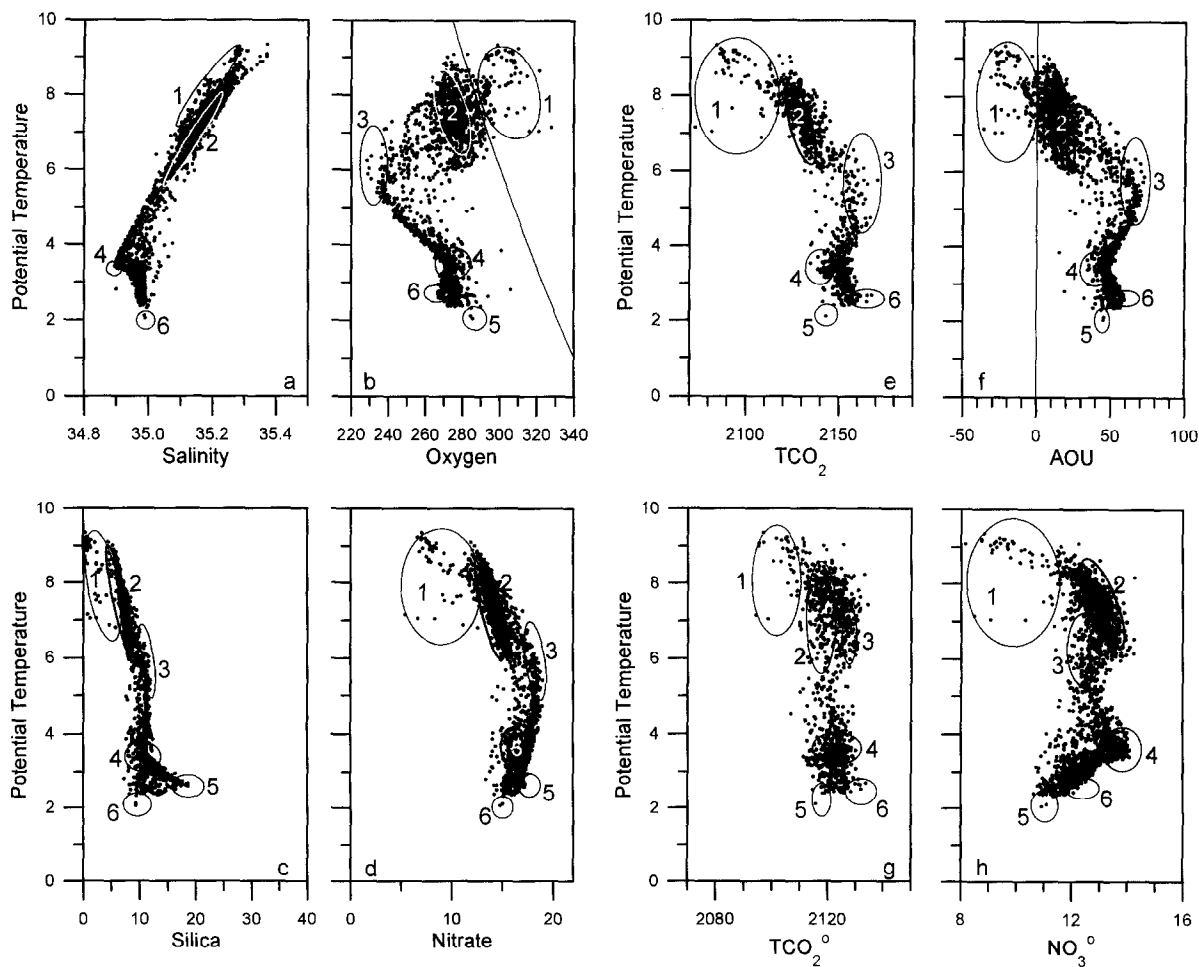


Fig. 3. As Fig. 2 for all samples on sections A to J in the Iceland Basin.

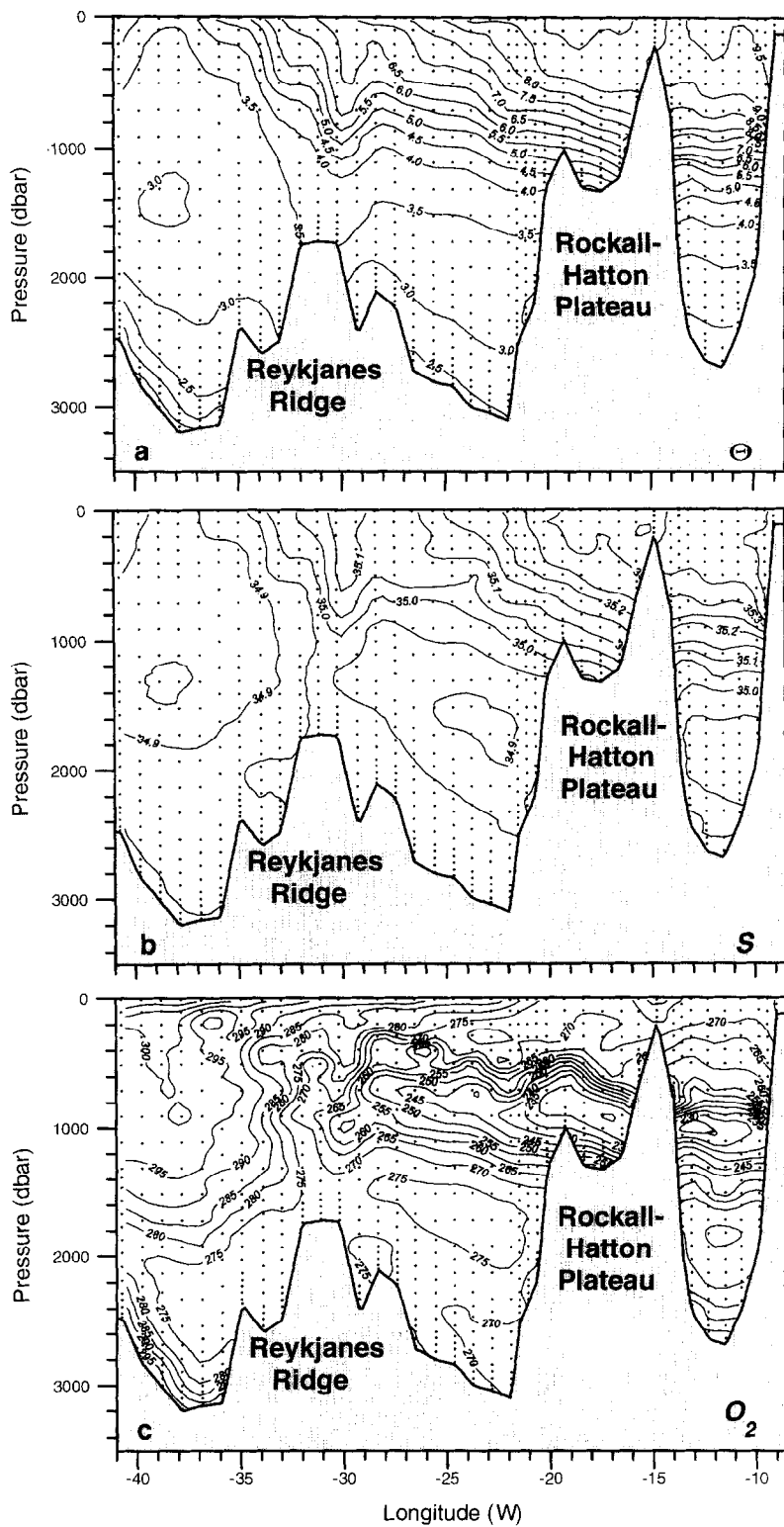


Fig. 4. Vertical distribution of: (a)  $\theta$  ( $^{\circ}\text{C}$ ); (b)  $S$ ; (c)  $\text{O}_2$  ( $\mu\text{mol kg}^{-1}$ ); (d)  $\text{TCO}_2$  ( $\mu\text{mol kg}^{-1}$ ); and (e)  $\text{AOU}$  ( $\mu\text{mol kg}^{-1}$ ) along the zonal section AR7E at a nominal latitude of 58°N.



Channel and the Iceland Basin (Figs. 4a, b and 5a, b). Salinity and  $\theta$  of SPMW range from slightly over 35.35 and over 9°C in the Rockall Channel, 35.25–35.3 and 8.5–9°C over the Rockall Hatton Plateau, 35.1–35.25 and 6–9°C in the Iceland Basin, and 34.9–34.95 and 3.5–4°C in the Irminger Sea (Figs. 2 and 3a, 4a, b and 5a, b), respectively. In the centre of the Irminger Sea SPMW appeared to be absent due to the doming of the very cold Labrador Sea Water concurring with the cyclonic circulation in this basin. SPMW appeared to be slightly undersaturated in  $O_2$  with an AOU of 10–20  $\mu\text{mol kg}^{-1}$ . The nutrient concentrations of the SPMW, although

slightly higher than in the SW, were relatively low (Figs. 2c, d and 3c, d) with typical values of  $\sim 5$ –10  $\mu\text{mol kg}^{-1}$  for Si and 11.5–16  $\mu\text{mol kg}^{-1}$  for  $\text{NO}_3$ . Comparison of the data presented here with data from a DUTCH-WARP cruise in this region in late summer 1990 suggests the presence of a small but significant seasonal signal in  $O_2$ ,  $\text{NO}_3$  and  $\text{TCO}_2$  (Van Aken, submitted).

### 3.2. Intermediate layers

In the permanent thermocline below the SPMW Intermediate Water (IW, 3) is found east of the

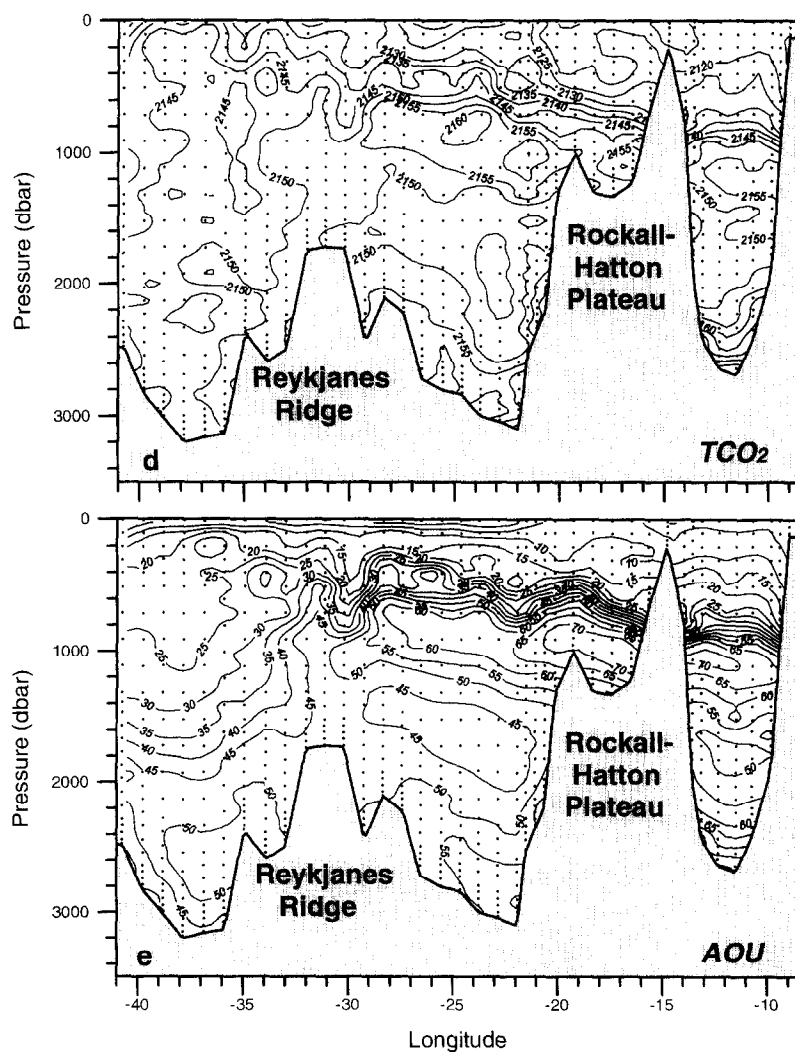


Fig. 4 (continued).

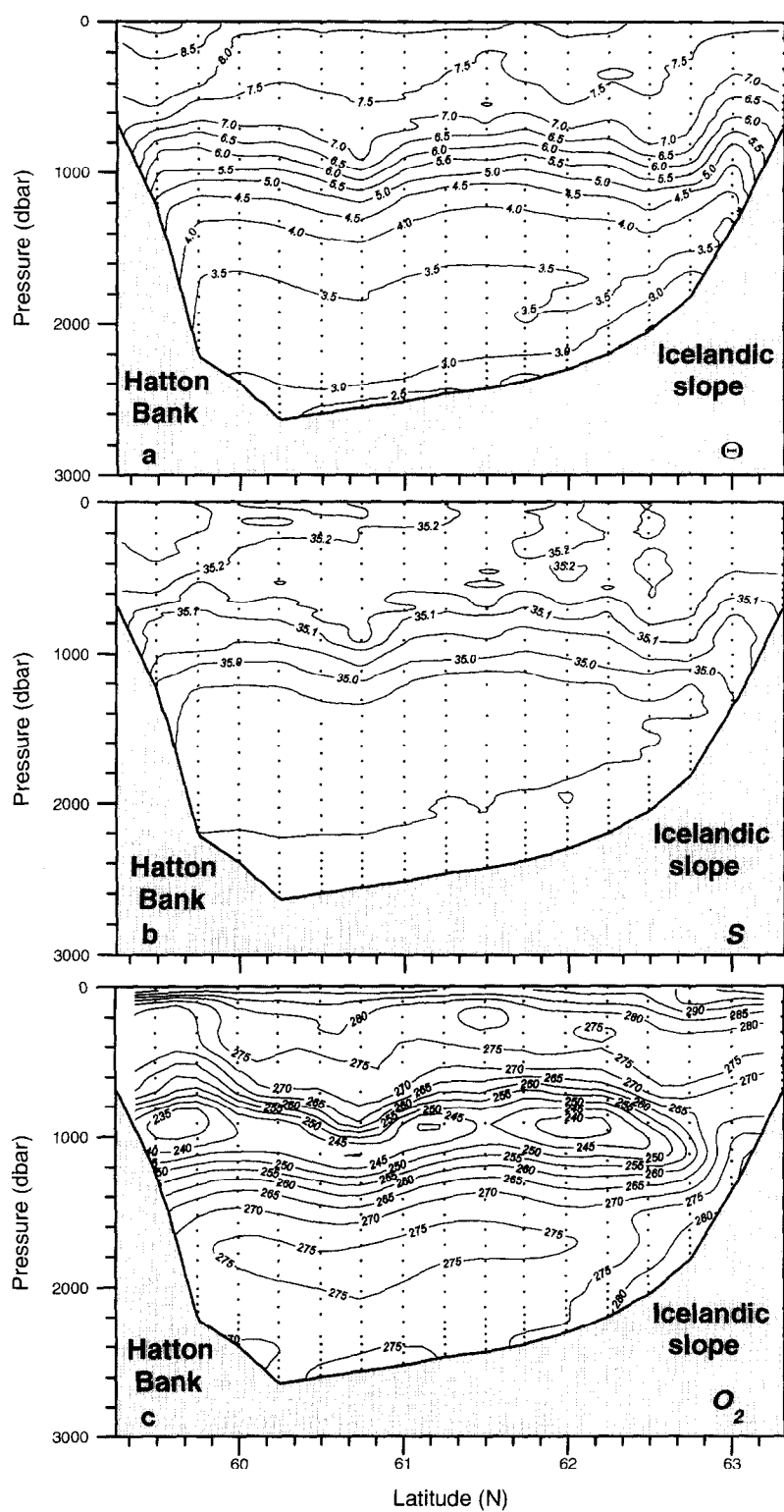


Fig. 5. As Fig. 4 along the meridional section F at 17°W.

Reykjanes Ridge with characteristic low values in  $O_2$  (Figs. 2b, 3b, 4c and 5c) and relatively high values for the nutrients (Figs. 2c, d and 3c, d). But in a  $\Theta$ – $S$  plot (Figs. 2 and 3a) IW does not show such typical extremes. The distinct bio-geochemical signal with the absence of characteristic extreme  $\Theta$  or  $S$  values in IW suggest mineralization of organic matter in the permanent thermocline as the cause of its characteristics (Tsuchiya et al., 1992; Van Aken and De Boer, 1995).

In volume the most important water type in the

Iceland Basin and the Rockall Channel is the Labrador Sea Water (LSW, 4) which is formed in the Labrador Sea by deep convection and reaches the eastern North Atlantic due to advection while it becomes modified due to diapycnal mixing (Talley and McCartney, 1982; Van Aken and De Boer, 1995). LSW in the Iceland Basin is characterized by a salinity minimum (Figs. 2 and 4b and 5b), relatively high  $O_2$  values (Figs. 3b, 4c and 5c), and intermediate nutrient concentrations (Fig. 3c, d). In the centre of the Irminger Sea even lower  $S$  and  $\Theta$

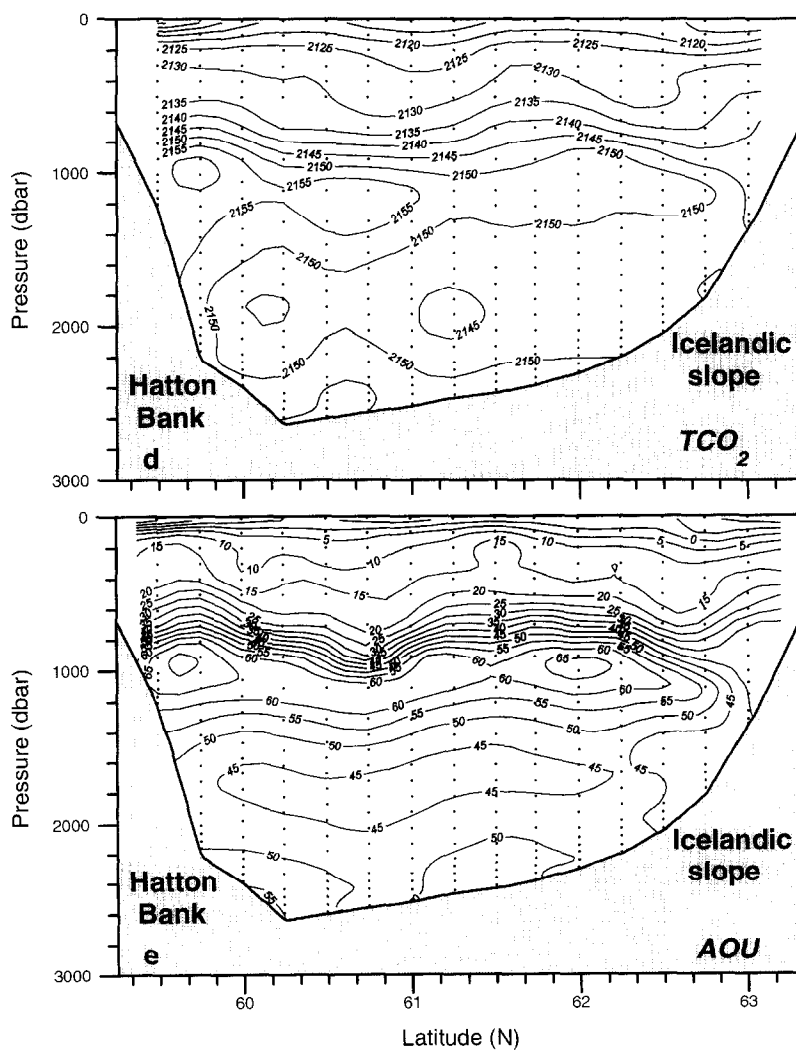


Fig. 5 (continued).

values are observed in the LSW core between 1000 and 1300 dbar,  $< 34.85$  and  $< 3.5^{\circ}\text{C}$  respectively (Fig. 4a, b).

### 3.3. Deep water in the Iceland Basin and Rockall Channel

In the near-bottom layers of both the Iceland Basin and the Irminger Sea competing cold water types are observed. Iceland–Scotland Overflow Water (ISOW, 5) enters the Iceland Basin by overflow across the sill on the Iceland–Scotland Ridge (Harvey and Theodorou, 1986; Van Aken and Eisma, 1987; Van Aken and De Boer, 1995), while Lower Deep Water (LDW, 6) is observed in The Rockall Channel and also enters the Iceland Basin (McCartney, 1992). Whereas ISOW is characterized by relatively high  $S$ , high  $\text{O}_2$  and low nutrient values LDW shows opposite characteristics (Fig. 3a–d). The low  $S$  of LDW (Fig. 2a) is assumed to be caused by a high content of Antarctic Bottom Water (AABW; McCartney, 1992) which, at least partly, is also responsible for the extremely high Si concentration of LDW. But whereas the original AABW is characterized by high  $\text{O}_2$  values, LDW has a low  $\text{O}_2$  concentration due to re-mineralization during the long time it takes for AABW to reach the North-eastern Atlantic. The lowest  $\theta$  in ISOW, observed during our survey, was  $\sim 2.00^{\circ}\text{C}$ , indicating that even at our section I ISOW was already modified considerably by entrainment of overlying SPMW which even caused a temperature inversion on top of the ISOW layer (Fig. 5a; Van Aken and De Boer, 1995). In the Iceland Basin the ISOW is modified further by entrainment of LDW which is centred at a density level just overlying the ISOW core (Van Aken, 1995a). The volume flow of ISOW across the Iceland–Scotland Ridge is  $\sim 2.7$  Sv below  $\sigma_{\theta} = 27.80 \text{ kg m}^{-3}$  (1 Sv =  $10^6 \text{ m}^3 \text{ s}^{-1}$ ), and increases to 3.5 Sv south of Iceland (Dickson et al., 1990; Saunders, 1993; Dickson and Brown, 1994; Van Aken, 1995b).

### 3.4. Deep water in the Irminger Sea

In the Irminger Sea ISOW which has left the Iceland Basin through the Charlie–Gibbs Fracture Zone as well as cold and fresher Denmark Strait Overflow Water (DSOW, 7) was observed. The re-

circulating ISOW in the Irminger Sea was characterized by a salinity maximum ( $S > 34.95$ ) near  $34^{\circ}\text{W}$  (Fig. 4b) as well as by a relatively low  $\text{O}_2$  values ( $< 275 \mu\text{mol kg}^{-1}$ , Fig. 4c). DSOW, characterized by low temperatures ( $\theta < 2^{\circ}\text{C}$ ), low nutrient values, and high  $\text{O}_2$  values (Fig. 2a–d) is transported from the overflow sill in Denmark Strait along the Greenland slope (Fig. 4a, b). The characteristic AOU value for DSOW is  $\sim 40 \mu\text{mol kg}^{-1}$ . DSOW is modified by entrainment of overlying ISOW and LSW which increases its volume transport below  $\sigma_{\theta} = 27.80 \text{ kg m}^{-3}$  from  $\sim 3$  Sv in Denmark Strait to  $\sim 12$  Sv at the latitude of our AR7E section (Dickson et al., 1990).

## 4. The hydrographic signature of $\text{TCO}_2$

In order to assess the importance of the conditioning of the water types during their initial formation due to air–sea interaction for the water type characteristics we have used the concept of preformed concentrations (Broecker and Peng, 1982). The newly formed water types are assumed to have biogeochemical characteristics equal to the preformed values, and their  $\text{O}_2$  concentrations are assumed to be the saturation value, in equilibrium with the atmosphere. Subsequent changes of these properties are due to ageing of the water types. Transport of the preformed  $\text{TCO}_2$  ( $\text{TCO}_2^0$ ) represents the “physical pump” for the oceanic conveyor belt. The deviations of  $\text{TCO}_2$  relative to  $\text{TCO}_2^0$  are caused by the “biological pump” (mineralization of organic matter) and also may contribute to the meridional carbon transport.

The  $\text{TCO}_2$  concentration of a water particle is modified by air–sea gas exchange, formation or dissolution of  $\text{CaCO}_3$ , primary production and mineralization of organic matter. In the latter two processes changes in  $\text{TCO}_2$  are accompanied by similar changes in  $\text{O}_2$ ,  $\text{PO}_4$ , and  $\text{NO}_3$ , assumed to be proportional to the “Redfield ratio”:

$$\text{P:N:C:O}_2 = 1:16:106:-138 \quad (1)$$

(Redfield et al., 1963). From a rigorous analysis of nutrient,  $\text{O}_2$  and  $\text{TCO}_2$  data on isopycnal surfaces, Takahashi et al. (1985) deduced a different Redfield ratio for the Atlantic Ocean. Taking data from sub-

surface isopycnals ( $\sigma_\theta = 27.0$  and  $27.2 \text{ kg m}^{-3}$ ) from the TTO-NAS and GEOSECS expeditions they showed that for this region the classic Redfield ratio underestimates  $\text{O}_2$  and overestimates the carbon effect. They gave a revised Redfield ratio for the Atlantic Ocean to be:

$$\text{P:N:C:O}_2 = 1:16:103:-172 \quad (2)$$

Fanning (1992) with a different approach used N:P ratios to divide and characterize the oceans into so-called “nutrient provinces” and estimated a N:P ratio of 14.7 for the Atlantic Ocean. For our purposes we want to use a “local” Redfield ratio, applicable to our northern North Atlantic data set. In order to determine the C:O<sub>2</sub> ratio we have calculated the apparent oxygen utilization (AOU) values along the AR7E section, defined by:

$$\text{AOU} = \text{O}_2(\text{saturation at } \theta, S) - \text{O}_2(\text{measured}) \quad (3)$$

From these data as well as from the  $\text{PO}_4$ ,  $\text{NO}_3$ , and  $\text{TCO}_2$  data we have determined mean profiles of these parameters for the stations along section AR7E (Fig. 6). These basin wide mean profiles clearly show the large scale ageing of the waters below the permanent thermocline by mineralization of organic matter; high values of AOU,  $\text{PO}_4$ ,  $\text{NO}_3$  and  $\text{TCO}_2$  below 1000 dbar. In plots of  $\text{PO}_4$ ,  $\text{NO}_3$ , and  $\text{TCO}_2$  from these mean profiles vs. AOU it is clearly visible that on a large scale the parameters are highly correlated (Fig. 7). With a linear regression we have estimated the ratios of changes of  $\text{PO}_4$ ,  $\text{NO}_3$ , and  $\text{TCO}_2$  vs. changes of AOU to be  $0.0062 \pm 0.0006$ ,  $0.088 \pm 0.006$ , and  $0.62 \pm 0.02$ , respectively. These ratios do not differ significantly from the ratios 1:172, 14.7:172 and 103:172 as actually plotted in Fig. 7. For the description of our data from the northern North Atlantic we therefore will use a locally valid Redfield ratio, by combining the results of Takahashi et al. (1985) and Fanning (1992) according to:

$$\text{P:N:C:O}_2 = 1:14.7:103:-172 \quad (4)$$

With this Redfield ratio it is possible to separate the original characteristics of water types from the bio-geochemically induced changes induced by mineralization of organic matter during the ageing of the water types. This is performed by the definition of

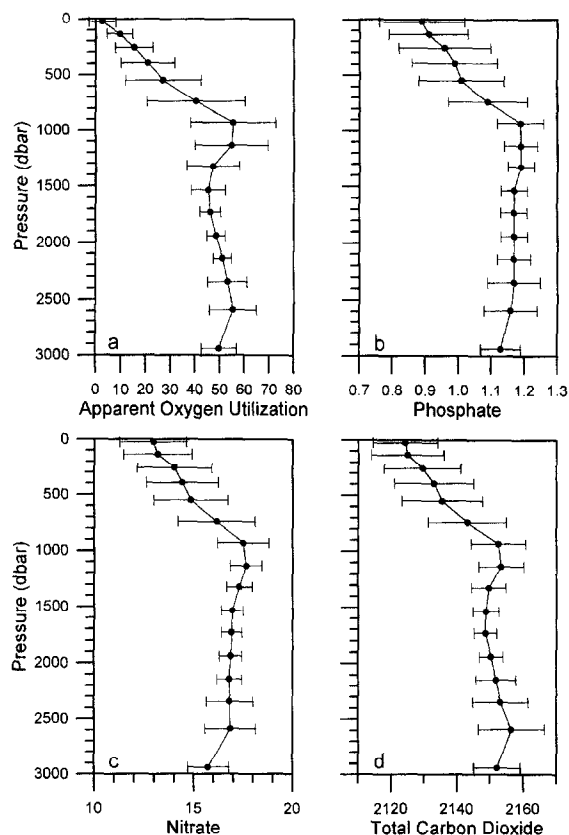


Fig. 6. Mean profiles of: (a) apparent oxygen utilization; (b) dissolved phosphate; (c) nitrate; and (d) total carbon dioxide, obtained by zonal averaging along section AR7E. The error bars indicate the standard deviation. All units are in  $\mu\text{mol kg}^{-1}$ .

preformed concentrations of, for example,  $\text{NO}_3$  and  $\text{TCO}_2$ , by:

$$\text{NO}_3^0 = \text{NO}_3 - (14.7/172) \cdot \text{AOU} \quad (5a)$$

$$\text{TCO}_2^0 = \text{TCO}_2 - (103/172) \cdot \text{AOU} \quad (5b)$$

$\text{TCO}_2^0$  and  $\text{NO}_3^0$  are assumed to be representative for the conditions when the original water types were formed near the sea surface due to air–sea interaction.

Whereas the SW had a near zero value for AOU on the AR7E section in mid-April with a slight tendency to decrease with time and sea surface temperature (Fig. 4a, c), values down to  $-40 \mu\text{mol kg}^{-1}$  were observed in the Iceland Basin during the spring bloom in early May (Figs. 3f and 5e). The latter coincided with extremely low  $\text{TCO}_2$  values

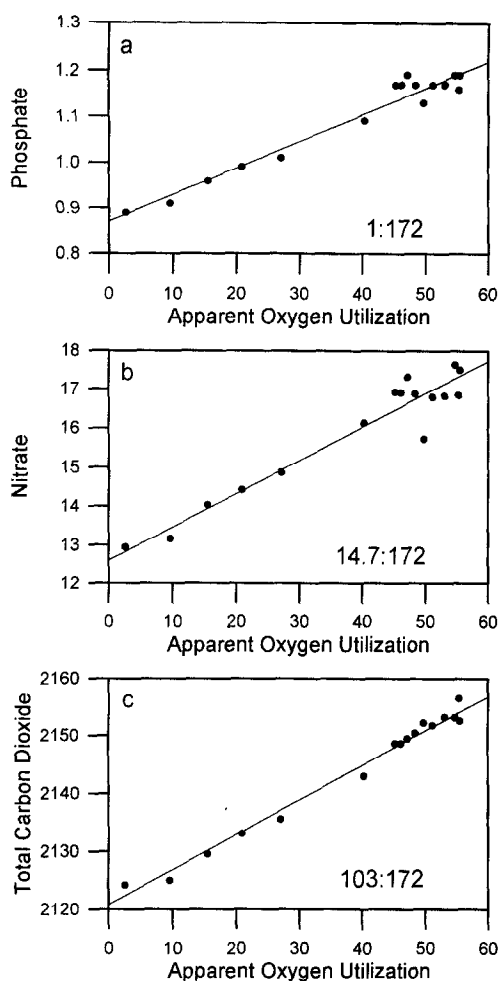


Fig. 7. Plots of: (a) dissolved phosphate; (b) nitrate; and (c) total carbon dioxide, vs. apparent oxygen utilization at AR7E from basin-wide averaged property profiles. The *straight lines* indicate the expected element ratios according to Eq. 4. The ratios, estimated by regression are virtually identical (see text). When doing regression for all data, rather than for basin-wide averages, the same ratios were also found. All units are  $\mu\text{mol kg}^{-1}$ .

near the sea surface (Figs. 3e and 5d) as well as with the low nutrient values (Fig. 3c, d).

The preformed values  $\text{NO}_3^0$  and  $\text{TCO}_2^0$  in SW appeared to be negatively correlated with the sea surface temperature (not shown), the latter with a regression coefficient of  $d\text{TCO}_2^0/dT = -4 \mu\text{mol kg}^{-1} \text{ } ^\circ\text{C}^{-1}$ . This value is about half the value which can be expected from the temperature-dependent saturation value alone, according to the model of Takahashi et al. (1993). The low value of the regression

coefficient probably reflects the effect of alkalinity (not measured) on the solubility of  $\text{CO}_2$ , as well as the slow response of the  $\text{TCO}_2$  content of surface water to changing environmental conditions, due to the inorganic chemistry of seawater (Keeling and Shertz, 1992). Broecker and Peng (1982) stress that, contrary to  $\text{O}_2$ , the typical adjustment time of  $\text{TCO}_2$  in surface waters is about one year. This will cause  $\text{TCO}_2^0$  to deviate from the actual saturation value of  $\text{TCO}_2$ . In the SPMW below the surface layer  $\text{TCO}_2$  varied between 2110 and 2140  $\mu\text{mol kg}^{-1}$  whereas AOU in SPMW varied from 5 to 20  $\mu\text{mol kg}^{-1}$ .

The IW was characterized by maxima in both  $\text{TCO}_2$  and AOU up to 2170 and 70  $\mu\text{mol kg}^{-1}$  respectively (Figs. 2e, f; 3e, f; 4d, e; and 5d, e). Below the IW core both  $\text{TCO}_2$  and AOU decreased toward the level where LSW was found ( $\theta = 3.4^\circ\text{C}$ ). There characteristic  $\text{TCO}_2$  and AOU values were 2141 and 41  $\mu\text{mol kg}^{-1}$ , respectively, in the Iceland Basin (Fig. 5) with even lower values in the Irminger Sea, especially for AOU (down to 25  $\mu\text{mol kg}^{-1}$ ; Fig. 4). These low values suggest very recent formation of the LSW, observed in the Irminger Sea. In the near-bottom layers high values of  $\text{TCO}_2$  and AOU were observed in the LDW core, low values in the DSOW core and intermediate values in the ISOW core (Fig. 2e, f).

The preformed parameters  $\text{TCO}_2^0$  and  $\text{NO}_3^0$  are shown in Figs. 2g, h and 3g, h. From a regression analysis it appears that on average  $\text{TCO}_2^0$  increases with 1.4  $\mu\text{mol kg}^{-1}$  per degree temperature decrease. This is about a factor 5 less than can be expected from the effect of temperature alone on the solubility of  $\text{CO}_2$  (Takahashi et al., 1993). As with the SW we ascribe this to the compensating role of alkalinity (Takahashi et al., 1993) and the deviation of  $\text{TCO}_2^0$  from the saturation value of  $\text{TCO}_2$  during water type formation due to the slow response of the sea surface  $\text{TCO}_2$  to the changing environmental conditions preceding the formation of the water types (Broecker and Peng, 1982). Alkalinity data, obtained from the Iceland Basin near  $60^\circ\text{N}$ ,  $20^\circ\text{W}$  in 1989 and 1990 (Stoll, 1994) and TTO data from the Iceland Basin indicate that alkalinity may explain 20–50% of this effect, according to the  $\text{TCO}_2$  saturation model of Takahashi et al. (1993). The result is that  $\text{TCO}_2^0$  has much less hydrographic structure than  $\text{TCO}_2$  (Figs. 2e, g and 3e, g) and that the vertical

gradient in  $\text{TCO}_2$  is mainly caused by the ageing by mineralization of the water types after their formation, rather than by significant differences in solubility in their formation areas. Contrary to  $\text{TCO}_2^0$ ,  $\text{NO}_3^0$  shows a definite hydrographic structure (Figs. 2h and 3h).

## 5. $\text{TCO}_2$ transport and the hydrographic structure

From the relation between the hydrographic structure and the  $\text{TCO}_2$  distribution qualitative information on the advective transport of dissolved inorganic carbon in the northern North Atlantic Ocean may be derived. Since the depths of the sills in Denmark Strait and on the Iceland–Scotland Ridge are quite shallow (500–800 m) only SW and SPMW are assumed to enter the Nordic Seas from the North Atlantic (Van Aken, 1995b). Deep return flows of high-density DSOW and ISOW across these sills, are driven by density differences. They transport water, which has been modified by air–sea interaction in the Nordic Seas. This implies that for the advection of IW, LSW and LDW the Irminger Sea, Iceland Basin and Rockall Channel are more or less dead ends. These water types are expected only to recirculate in these basins. Therefore their characteristic  $\text{TCO}_2$  content will not contribute to an advective meridional flux of dissolved inorganic carbon. Mixing of IW, LSW and LDW with neighbouring water types only contributes to the maintenance of the observed  $\text{TCO}_2$  structure, not to the meridional advective transport.

We may take the mean early spring value for  $\text{TCO}_2$  in the SPMW in the Iceland Basin and Rockall Channel of  $2110\text{--}2120\text{ }\mu\text{mol kg}^{-1}$  to be representative for the warm and saline Atlantic water (Fig. 4d) leaving the Northeastern Atlantic across the Iceland–Scotland Ridge. For the ISOW which flows southwards we choose  $2142\text{ }\mu\text{mol kg}^{-1}$  as characteristic value observed on section I near the Iceland–Scotland Ridge and apply this value also as characteristic for DSOW in Denmark Strait. As described above the total thermohaline overturning of Atlantic water through the Nordic Seas and its transformation to DSOW and ISOW amounts to the order of 5.7 Sv. The inflow of Atlantic water to the Nordic Seas is  $\sim 4$  Sv higher. However, this water is not

involved in the large-scale thermohaline overturning but leaves the Nordic Seas again as a near-surface flow in the East Greenland Current (Hopkins, 1991). With a total thermohaline overturning of 5.7 Sv, and a  $\text{TCO}_2$  difference between the north and south flowing water of  $27\text{ }\mu\text{mol kg}^{-1}$ , this process will result in a southward total baroclinic  $\text{TCO}_2$  transport of nearly  $-0.16 \cdot 10^6\text{ mol s}^{-1}$  ( $-0.06\text{ Gt a}^{-1}\text{ C}$ ). This number is definitely smaller than the total advective transport, estimated by Brewer et al. (1989) across a zonal section near  $25^\circ\text{N}$  to amount to  $-0.7 \cdot 10^6\text{ mol s}^{-1}$  ( $-0.26\text{ Gt a}^{-1}\text{ C}$ ). Ours is admittedly a rather crude estimate, which does not take into account the possible lateral eddy correlation between the laterally varying  $\text{TCO}_2$  and velocities, either barotropic or baroclinic. It therefore leaves out the possible contribution of the East Greenland Current. Concentration of the northward transport of SW and SPMW in the eastern part of section AR7E where the lowest  $\text{TCO}_2$  values were observed (Fig. 4d) and cyclonic recirculation of the surface flow in the Iceland Basin (Otto and Van Aken, 1996) will lead to a southward transport of dissolved inorganic carbon. In the deep Iceland Basin as well as in the Irminger Sea the deep cyclonic re-circulation will support a northward carbon transport. This being said, the hydrographic transport model of Brewer et al. (1989) is not necessarily more accurate than ours, whereas our  $\text{TCO}_2$  data have rather high accuracy and give a better coverage of a cross-Atlantic zonal section. More importantly, the  $25^\circ\text{N}$  section of theirs would also include any contributions to the North Atlantic deep-water complex from formation waters of the Labrador Sea. Consequently, one would expect the net southward flux at  $25^\circ\text{N}$  to be larger than at our section, as apparently is the case ( $-0.7 \cdot 10^6\text{ mol s}^{-1}$  vs.  $-0.16 \cdot 10^6\text{ mol s}^{-1}$ ). The difference between these transports agrees at least in order of magnitude with the  $\text{CO}_2$  uptake in the North Atlantic sub-tropical gyre as estimated by Tans et al. (1990) to be  $0.8 \cdot 10^6\text{ mol s}^{-1}$  ( $0.3\text{ Gt a}^{-1}\text{ C}$ ). In any case a more elaborate determination of the total transport is required in order to come to a reliable estimate of the total exchange of dissolved inorganic carbon between the North Atlantic and the Nordic Seas as discussed by Stoll et al. (1996–this issue).

As discussed above, most hydrographic structure of the  $\text{TCO}_2$  distribution is linearly correlated with

the AOU, and therefore caused by bio-geochemical processes (primary production and mineralization of organic matter). The original  $\text{CO}_2$  content of the water types, reflected by the preformed  $\text{TCO}_2^0$  (Fig. 2g), indicates a difference between the SPMW in the Iceland Basin and ISOW/DSOW of  $\sim 8 \mu\text{mol kg}^{-1}$ . This implies that the thermohaline overturning transport of dissolved inorganic carbon, due to the preformed  $\text{CO}_2$  content, is about one-third of the transport value, given above. In the calculation of  $\text{TCO}_2^0$  we used the Takahashi stoichiometry  $\text{C}:\text{O}_2 = 103:-172$  according to Eq. (4) in keeping with our observations (Fig. 7). When using the classic Redfield ratio  $\text{C}:\text{O}_2 = 106:-138$  according to Eq. (1) for the calculation of  $\text{TCO}_2^0$  the difference between SPMW and ISOW/DSOW amounts only to  $\sim 3 \mu\text{mol kg}^{-1}$  implying an even smaller transport of preformed  $\text{CO}_2$ . So subduction of inorganic carbon by the convective processes which form the original water types, the physical pump, seems to be of minor importance for the generation of the mean vertical  $\text{TCO}_2$  gradient. Most of the vertical differences of  $\text{TCO}_2$  are probably caused by the mineralization of organic matter, originating from algal blooms in the surface layer. This reflects the importance of the biological pump for the generation of the hydrographic structure which supports the advective meridional baroclinic carbon flux in the northern North Atlantic, close to the overflow sills.

## Acknowledgements

We are indebted to the captain, officers and crew of RV "Tyro" for their pleasant cooperation during the cruise. The coulometric determinations could not have been done without the help, advice and encouragement of Professor P.J. LeB. Williams, and Dr. C. Robinson. This research was supported by the Marine Research Foundation (SOZ), subsidiary of the Foundation for Netherlands Scientific Research (NWO). Additional funding was given by the Carbon Dioxide Research Division, also subsidiary of NWO; and the ministry of Health, Urban Planning and Environment (VROM). This is NIOZ publication 3020.

## References

- Brewer, P.G., Goyet, C. and Dyrssen, D., 1989. Carbon dioxide transport by ocean currents at 25°N latitude in the Atlantic Ocean. *Science*, 246: 477–479.
- Broecker, W.S. and Peng, T.-H., 1982. *Tracers in the sea*. Columbia University Press, Palisades, NY, 690 pp.
- Broecker, W.S. and Peng, T.-H., 1992. Interhemispheric transport of carbon dioxide by ocean circulation. *Nature (London)*, 356: 587–589.
- Chen, C.-T.A., Jones, E.P. and Lin, K., 1990. Wintertime total carbon dioxide measurements in the Norwegian and Greenland seas. *Deep-Sea Res.*, 37: 1455–1473.
- Dickson, R.R. and Brown, J., 1994. The production of North Atlantic Deep Water: sources, sinks, and pathways. *J. Geophys. Res.*, 99: 12319–12314.
- Dickson, R.R., Gmitrowicz, E.M. and Watson, A.J., 1990. Deep-water renewal in the northern North Atlantic. *Nature (London)*, 344: 848–850.
- Fanning, K.A., 1992. Nutrient provinces in the sea: Concentration ratios, reaction rate ratios, and ideal covariation. *J. Geophys. Res.*, 97: 5693–5712.
- Harvey, J.G. and Theodorou, A., 1986. The circulation of Norwegian Sea overflow water in the eastern North Atlantic. *Oceanol. Acta*, 9: 393–402.
- Hopkins, T.S., 1991. The GIN Sea: A synthesis of its physical oceanography and literature review 1972–1985. *Earth-Sci. Rev.*, 30: 175–318.
- Johnson, K.M., Williams, P.J. LeB., Brändström, L. and Sieburth, J.McN., 1987. Coulometric total carbon dioxide analysis for marine studies: Automation and calibration. *Mar. Chem.*, 21: 117–133.
- Keeling, R.F. and Shertz, S.R., 1992. Seasonal and interannual variations in atmospheric oxygen and implications for the global carbon cycle. *Nature (London)*, 358: 723–727.
- Martel, F. and Wunsch, C., 1993. The North Atlantic circulation in the early 1980s — An estimate from inversion of a finite difference model. *J. Phys. Oceanogr.*, 23: 898–924.
- McCartney, M.S., 1992. Recirculating components to the deep boundary currents of the northern North Atlantic. *Progr. Oceanogr.*, 29: 283–383.
- McCartney, M.S. and Talley, L.D., 1982. The Subpolar Mode Water of the North Atlantic Ocean. *J. Phys. Oceanogr.*, 12: 1169–1188.
- Otto, L. and Van Aken, H.M., 1996. Surface circulation in the North-east Atlantic as observed with drifters. *Deep-Sea Res.* (in press).
- Redfield, A.C., Ketchum, B.H. and Richards, F.A., 1963. The influence of organisms on the composition of sea water. In: M.N. Hill (Editor), *The Sea*, Vol. 2. Wiley-Interscience, New York, NY, pp. 26–77.
- Robinson, C. and Williams, P.J. LeB., 1991. Development and assessment of an analytical system for the accurate and continual measurement of total dissolved inorganic carbon. *Mar. Chem.*, 34: 157–175.
- Saunders, P.M., 1993. The flux in the dense overflow south of Iceland. *Ann. Geophys.* 11(Suppl. 2): C142.



- Stoll, M.H.C., 1994. Inorganic carbon behaviour in the North Atlantic Ocean. Ph.D. Thesis, Groningen University, Groningen, 193 pp.
- Stoll, M.H.C., Rommets, J.W. and De Baar, H.J.W., 1993. Effects of selected calculation routines and dissociation constants on the determination of total carbon dioxide in seawater. *Deep-Sea Res.*, 40: 1307–1322.
- Stoll, M.H.C., Van Aken, H.M., De Baar, H.J.W. and De Boer, C.J., 1996. Meridional carbon dioxide transport in the northern North Atlantic. *Mar. Chem.*, 55: 205–216.
- Takahashi, T.J., Broecker, W.S. and Langer, S., 1985. Redfield ratio based on chemical data from isopycnal surfaces. *J. Geophys. Res.*, 90: 6907–6924.
- Takahashi, T.J., Olafsson, J.G., Chipman, D.W. and Sutherland, S.C., 1993. Seasonal variation of CO<sub>2</sub> and nutrients in the high latitude surface oceans: A comparative study. *Global Biogeochem. Cycles*, 7: 843–878.
- Talley, L.D. and McCartney, M.S., 1982. Distribution and circulation of Labrador Sea water. *J. Phys. Oceanogr.*, 12: 1189–1205.
- Tans, P.P., Fung, I.Y. and Takahashi, T., 1990. Observational constraints on the global atmospheric CO<sub>2</sub> budget. *Science*, 247: 1431–1438.
- Tsuchiya, M., Talley, L.D. and McCartney, M.S., 1992. An eastern Atlantic section from Iceland southward across the equator. *Deep-Sea Res.*, 39: 1885–1917.
- Van Aken, H.M., 1992. DUTCH-WARP 91: Tyro cruise 91/1, Part 1, WOCE Hydrographic Program section AR7E (cruise report). NIOZ, Den Burg/Texel, 34 pp. + figs.
- Van Aken, H.M., 1995a. Hydrographic variability in the bottom layer of the Iceland Basin. *J. Phys. Oceanogr.*, 25: 1716–1722.
- Van Aken, H.M., 1995b. Mean currents and current variability in the Iceland Basin. *Neth. J. Sea Res.*, 33: 135–145.
- Van Aken, H.M. and De Boer, C.J., 1995. On the synoptic hydrography of intermediate and deep water masses in the Iceland Basin. *Deep-Sea Res.*, 42: 165–189.
- Van Aken, H.M. and Eisma, D., 1987. The circulation between Iceland and Scotland derived from water mass analysis. *Neth. J. Sea Res.*, 21: 1–15.